SIMPLE EVOLUTIONARY STRUCTURAL OPTIMIZATION FOR MULTIPLE MATERIALS

JAROSLAV ROJICEK, DAGMAR LICKOVA

VSB – Technical University of Ostrava, Department of Applied Mechanics , Ostrava, Czech Republic

DOI: 10.17973/MMSJ.2021_10_2021090

Jaroslav.rojicek@vsb.cz

An evolutionary procedure for multiple materials is presented. A material is selected due to an allowable stress interval for the material. The presented method includes a mesh-independent filter. The proposed algorithm is applied to three examples with four or five materials. In the presented examples, the effect of an evolution rate, a filter setting, and the number of elements, are shown in a simplified way. It is shown that the final topology of structure meets the stress requirements of the materials.

KEYWORDS

FEA, ESO, Multiple materials, von Mises stress, Soft kill deactivation

1 INTRODUCTION

Topology optimization (TO) finds the best material distribution in a defined design domain. TO is often used to design components made by additive technology from a single material, see
[Paska 2020]. In TO, the Finite Element Method (FEM) is usually used for structure analysis. The most used TO methods for additive technology include Solid Isotropic Material with Penalization (SIMP) [Krishna 2017], Level set method [Qian 2020], Evolutionary Structural Optimization (ESO) [Huang 2010] and their modifications. Advances in additive manufacturing allow more printing materials to be used [Han 2010]. Modifications of the above methods for multiple materials can also be found in the literature (SIMP [Wang 2016], Level set method [Wang 2004], Bi-directional ESO [Huang 2009]).

The ESO method, published in its simple form [Xie 1993], uses the value of an equivalent stress in the element as a rejection criterion for topological optimization. We assumed that a typical product can include these materials: steel, aluminum or other alloys, plastic, or foam as the non-load-bearing material. We are able to easily determine or estimate Yield stress for a large number of these materials. Critical analysis of the ESO method and its comparison with other numerical methods of structural topology optimization shows [Rozvany 2009]. However, there are modifications to the method that overcome some of the shortcomings, for example [Gao 2020], and the method is still in use and evolving, see [Han 2021]. The method can provide a simplified view of a possible structure design topology.

In the following, the basic description of ESO method and a modified version of the ESO algorithm for multiple materials are presented. This modified version is applied to three simple examples and the results are briefly discussed.

2 EVOLUTIONARY STRUCTURAL OPTIMIZATION

The basic procedure for ESO was published on [Xie 1993]. The method uses a rejection criterion, such as the von Mises stress. Elements selected using the rejection criterion are removed from the structure, for example, if the von Mises stress in the element is less than a criterion value. The criterion value is calculated as a rejection ratio (RR) multiplied by the maximum von Mises stress over the structure. Initial value of the rejection ration is low, for example 1%. A Finite Element Analysis and element elimination are repeated in cycles with the same criterion value until a steady state is reached, that is, no element is selected for elimination. At this stage, an evolution rate (ER) is added to the rejection ratio and the interaction process continues. The evolution process ends if the rejection ratio reaches a predefined value, for example 25%.

3 EVOLUTIONARY STRUCTURAL OPTIMIZATION FOR MULTIPLE MATERIALS (MM ESO)

For application to multiple materials, the method briefly described in the previous chapter was modified. In the following text, the letter i will be used to denote the element number, the letter j to denote the material.

As a base for construction, the rejection criterion was taken non-averaged value of an equivalent element stress (σ_i), where subscript represents an element number. For the materials used in this paper can be applied the von Mises stress. The rejection criterion can be constructed from Yield stress for many materials (steel, aluminum alloy, etc.). For optimization, we can select, for example, 5 materials as are shown in Tab. 1. Selected materials will be further marked as follows (1, 2, 3, 4, 5), with reference to the corresponding table. The materials can be ordered by the allowable value of the stress (see Tab. 1).

j - Material	σ^j_{Min} [MPa]	σ^j_{Max} [MPa]
1 - Ti-6Al-4V	355	880
2 - s355J2	120	355
3 - AL EN AW 5005H14	10	120
4 - ABS M30	5	10
5 - Non-load-bearing material	0	5

Table 1. An example of allowable stress intervals for the materials

Where $\boldsymbol{\sigma^j_{Max}}$ is a maximum allowable stress for j-th material, for example Yield stress, $\boldsymbol{\sigma^j_{Min}}$ is the minimum allowable stress, where the value is taken taken as $\boldsymbol{\sigma^{j+1}_{Max}}$or 0 for the lowest material. Therefore, if the stress value for i-th element and j -th material is not within the interval ($\boldsymbol{\sigma^j_{Min}}$, $\boldsymbol{\sigma^j_{Max}}$), then the element is suitable for material change. The rejection ratio is base on a function $f(\sigma_i, j)$ and it is formulated as follows:

$$f(\sigma_i,j)=\begin{cases}(\sigma_i-\boldsymbol{\sigma^j_{Max}}),\ for\ \ \sigma_i>\boldsymbol{\sigma^j_{Max}},\\(\sigma_i-\boldsymbol{\sigma^j_{Min}}),\ for\ \ \sigma_i<\boldsymbol{\sigma^j_{Min}},\\0,\ \text{otherwise},\end{cases} \tag{1}$$

where σ_i is the equivalent stress for i-th element and j is the designation of its material. Initial material for all elements is the material with highest value of maximum allowable stress (for example, $j=1$). We assume that all elements of the initial structure satisfy the following:

$$0\le\sigma_i\le\boldsymbol{\sigma^1_{Max}},\ \text{therefore}\ \ \mathbf{0}\le|f(\sigma_i,1)|\le\boldsymbol{\sigma^1_{Min}} \tag{2}$$

Hence, the initial value of the rejection ratio is chosen as $\mathrm{RR}=\boldsymbol{\sigma^1_{Min}}$. The rejection criterion is defined as follows

$$\text{if}\ \ |f(\sigma_i,j)|>\mathrm{RR}\ \ \text{then modify material.} \tag{3}$$

The rejection criterion is checked in all elements of the current simulation and the material *j* of *i*-th element is changed based on the sign of $f(\sigma_i, j)$ as follows:

if $f(\sigma_i, j) > 0$ then $j = j - 1$ (4)

if $f(\sigma_i, j) < 0$ then $j = j + 1$ (5)

The following actions are very similar to the original method. A Finite element analysis and material modification is repeated in cycle with the same RR until a steady state is reached, but the number of cycles with the same RR is limited by the value N_R. At this stage, the evolution rate ER reduces RR value, as follows:

$\mathrm{RR} \leftarrow \mathrm{RR} - \mathrm{ER}$. (6)

A constant size of ER is a base choice. However, due to the different interval lengths used for the materials (see Tab. 1), the adaptive ER (AER) is designed as follows:

$\mathrm{AER}_j \leftarrow (\boldsymbol{\sigma}^{\mathbf{j}}_{\mathbf{Max}} - \boldsymbol{\sigma}^{\mathbf{j}}_{\mathbf{Min}})/\boldsymbol{N_\sigma}$. (7)

The AER value varies depending on the RR value with respect to the interval for each material. That is, if $\mathrm{RR} \in \langle \boldsymbol{\sigma}^{\mathbf{2}}_{\mathbf{Min}}, \boldsymbol{\sigma}^{\mathbf{2}}_{\mathbf{Max}} \rangle$ then AER_2 is used and $\boldsymbol{N_\sigma}$ is a number of interval divisions. The AER value is used instead of the ER value in Eqv. (6). Both approaches are tested in Example 1, AER is used in the other examples. The evolution process ends if the RR value is less than or equal to an allowable error of the results ($\mathrm{RR} \leq 0$).

3.1 *Mesh filter*

The article uses a filter published, for example, in [Huang 2010]. An equivalent element stress (σ_i) is used as a sensitivity number. An element position is defined by a center point of the element and its position, for i-th element it is (x_i, y_i, z_i). The effect of the k-th element on the i-th element is determined by the distance between them $(r_{i,k})$ as follows:

$$r_{i,k} = \sqrt{(x_i - x_k)^2 + (y_i - y_k)^2 + (z_i - z_k)^2}\,, \quad (8)$$

and is limited by the value of R. A weight factor $w(i,k)$ is formulated as follows :

$$w(i,k) = \begin{cases} (R - r_{i,k}), & for \quad r_{i,k} < R, \\ 0, & \text{otherwise.} \end{cases} \quad (9)$$

A filtered element stress value $\hat{\sigma}(\sigma_i, j)$ is defined as follows:

$$\hat{\sigma}_i = \frac{\sum_{k=1}^{M} w(i,k)\,\sigma_i}{\sum_{k=1}^{M} w(i,k)}\,, \quad (10)$$

where M is the total number of elements in the region defined by the radius R and the center at the center point of the i-th element. In Example 1, the filter is deactivated, Example 2 tests the effect of different values of R.

3.2 *MM ESO algorithm*

The problem can be simply described as:

$$\text{Minimize g} = \frac{\sum_{i=1}^{N_E} |f(\sigma_i, j)|}{N_E}\,, \quad (11)$$

where N_E is the number of elements and g is an objective function. The RR value was used as the termination criterion, and the objective function shows the average value of $|f(\sigma_i, j)|$ per element. For the information about the optimization process is presented a value of the structure weight $\mathbf{M}$. However, the weight of the structure has no effect on optimization. Other constraints, such as displacements, are not considered in the algorithm. A flowchart of the MM ESO method is shown in Fig. 1. The basic procedure is outlined below:

Step 1 : Definition of the initial structure including dimensions, materials, boundary conditions, mesh, etc.

Step 2 : Definition of all parameters or their initial values, such as material parameters, ER, RR, R, etc.

Step 3 : FEA.

Step 4 : The filter application and calculation the filtered element stress value $\hat{\sigma}_i$ and values of $f(\hat{\sigma}_i, j)$ for all elements.

Step 5 : Selection elements for material update by Eqv. (3).

Step 6 : Checking evolutionary criteria, if no elements are selected or the number of cycles with the same RR value exceeds N_R, then the algorithm proceeds to step 8. If any elements are selected, the algorithm proceeds to Step 7.

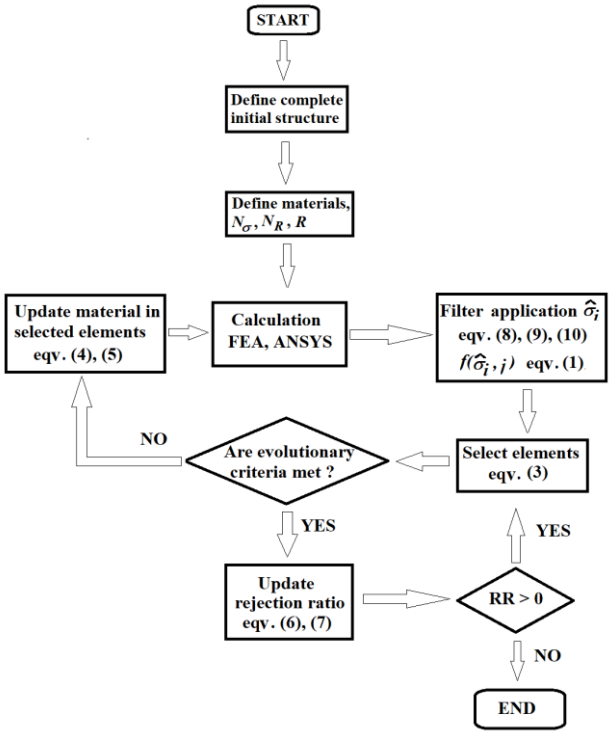

Figure 1. Schema of the MM ESO algorithm.

Step 7 : The material in the selected elements is updated according to the sign of the function $f(\hat{\sigma}_i, j)$, Eqv. (4), (5).

Step 8 : The rejection ratio is modified Eqv. (6) and ER or AER.

Step 9 : If the value of the rejection ratio is greater than zero, the algorithm proceeds to step 5, else the algorithm is terminated.

4 EXAMPLES

Three presented examples are 2D plates, the plate is fixed and loaded by a force on a few nodes. The behavior of the proposed algorithm is tested for different positions of fixed and loaded nodes. This boundary conditions are presented for each example in a separate figure. For testing was selected linear elastic material model for all materials. The materials are identified only by the number given in Tab 1. For analysis are used material parameters, namely Young's modulus (E), Poisson's ratio (μ), the material density (ρ), and Yield stress (Re). The value of $\boldsymbol{\sigma}^{\mathbf{j}}_{\mathbf{Min}}$ is determined by the selection of material for optimization, as explained in the previous chapter. The values of parameters for all materials are shown in Tab. 2. For the simulation of the plate is used software ®Ansys/APDL with SHELL181 element type [®Ansys 2015].

j	E [MPa]	μ [−]	ρ [kg/m^3]	Re [MPa]
1	104000	0,3	4429	880
2	210000	0,3	7850	355
3	70000	0,3	2700	120
4	1950	0,3	1000	10
5	0,1	0,3	10	1

Table 2. Material parameters for the materials

Example 1 shows the effect of changing the RR value depending on the method used. There were used two methods, a constant evolution rate ER and an adaptive evolution rate AER. Example 2 shows the selected results for four settings of the filter. Example 3 shows the effect of mesh quality and number of elements on the number of iterations during optimization.

4.1 Example 1

Example 1 is often used in the literature for topological optimization tasks (e.g., [Simonetti 2021]). Materials $(\mathbf{1}, \mathbf{2}, \mathbf{3}, \mathbf{4}, \mathbf{5})$ are used for optimization, and their parameters are shown in Tab. 1 and Tab. 2. The plate dimensions are $\boldsymbol{a} = \mathbf{160}\ [\mathbf{mm}]$, $\boldsymbol{b} = \mathbf{100}\ [\mathbf{mm}]$ and thickness $\boldsymbol{t} = \mathbf{1}\ [\mathbf{mm}]$, the loading force is $\boldsymbol{F} = \mathbf{3000}\ [\mathbf{N}]$, its position is shown in Fig. 2. The corners on the left side of the plate are fixed (see Fig. 2). However, due to condition (2), two outer nodes were always used to fix the plate.

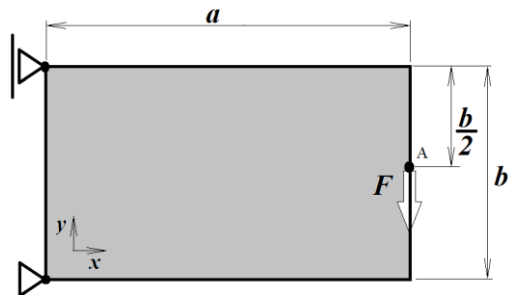

Figure 2. Example 1, dimensions and boundary conditions.

The side **a** was divided by 32 and side **b** by 20 and the total number of elements was $N_E = 640$. The setting of MM ESO algorithm was $N_R = 6$ and $R = 1\ [\mathrm{mm}]$. The results for first optimization with the constant size $\mathrm{ER} = 2$ and selected iteration number is shown in Fig. 3 and Tab. 3.

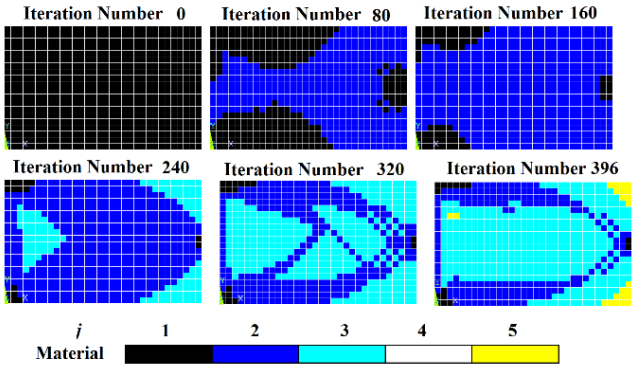

Figure 3. The evolution of structure topology, the constant size of ER.

Iteration Number	g [MPa]	M [kg]	RR [−]
0	254	0.071	355
80	112	0.103	271
160	48	0.119	211
240	21	0.110	61
320	3.2	0.080	25
396	2.4	0.066	-1

Table 3. The evolution of results properties with the constant size of ER.

The results for second optimization with the adaptive evolution rate AER ($\boldsymbol{N_\sigma} = 10$) is shown in Tab. 4. The results are nearly the same with a significantly lower iteration number. Fig. 4 shows the final topology structure with the equivalent stress ordered by the element material.

Iteration Number	g [MPa]	M [kg]	RR [-]
1	254	0.071	355
30	38	0.123	138
68	2.7	0.074	15
122	1.3	0.065	0

Table 4. The evolution of results properties with the adaptive evolution rate (AER).

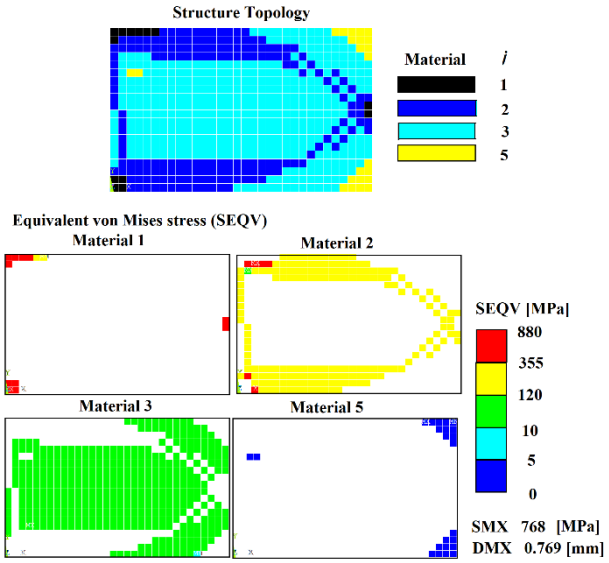

Figure 4. The last structure topology for AER and an equivalent Von Mises stress [MPa].

4.2 Example 2

Example 2 was inspired by [Simonetti 2021]. The plate dimensions are $\boldsymbol{a} = \mathbf{100}\ [\mathbf{mm}]$, and thickness $\boldsymbol{t} = \mathbf{1.5}\ [\mathbf{mm}]$, the loading force is $\boldsymbol{F} = \mathbf{12000}\ [\mathbf{N}]$, and its position is in the plane of symmetry in the upper corner. This symmetry was used for the simulation model as shown in Fig. 5, and the lower corner on the right side of the plate is fixed.

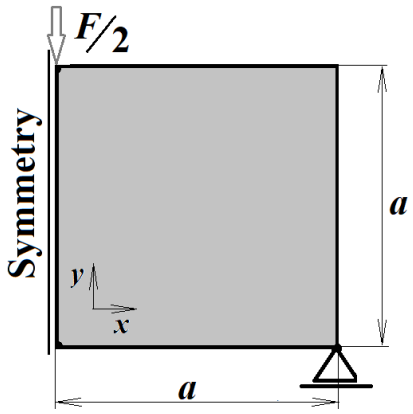

Figure 5. Example 2, dimensions and boundary conditions.

However, due to condition (2), the loading force was evenly distributed at three nodes (2000 + 2000 + 2000 [N]) and the stress concentration at the fixed node was reduced by adding two forces (2000 + 2000 [N]) in the y-axis direction at the nearest nodes at the bottom edge of plate.

Materials $(\mathbf{1},\mathbf{2},\mathbf{3},\mathbf{4})$ are used for optimization, and their parameters are shown in Tab. 2.

The side **a** was divided by 20 and the total number of elements was $N_E = 400$. The setting of MM ESO algorithm was $N_R = 10$, there was used AER ($\boldsymbol{N_\sigma} = 20$).

The structure optimization was performed for 4 setting values of R ($R = 1, R = 6, R = 8, R = 11$ [mm]).

R	g [MPa]	Iteration Number	M [kg]
1	1.57	221	0.073
6	0.68	124	0.071
8	0.74	110	0.071
11	1.94	99	0.071

Table 4. The effect of the *R* value of the filter on the optimization.

The final structure topology for the selected values *R* and their equivalent stresses are shown in Fig. 6.

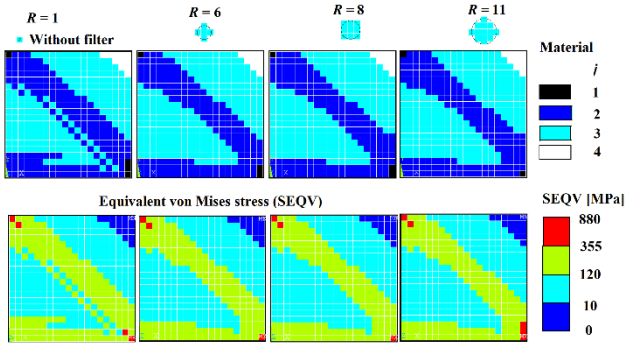

Figure 6. The last structure topology for a different setting of the filter and their equivalent Von Mises stress [MPa].

4.3 Example 3

A similar example can be found in [Simonetti 2021] again. The plate for example 3 has the same dimension as the example 1, $\boldsymbol{a = 160}$ [mm], $\boldsymbol{b = 100}$[mm], with a thickness $\boldsymbol{t = 1.5}$ [mm]. In this case, there is a hole in the plate with a diameter of $\boldsymbol{d = 30}$ [mm] and the coordinates of centre $\boldsymbol{c = 40}$ [mm] and $\boldsymbol{e = 100}$ [mm]. The situation is shown in Fig. 7.

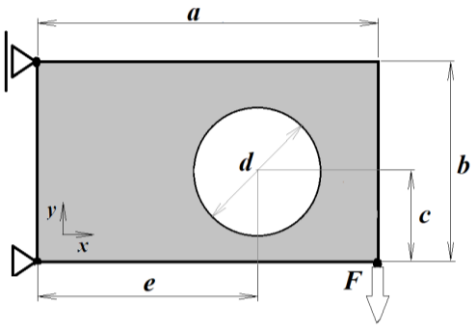

Figure 7. Example 3, dimensions and boundary conditions.

The loading force is $\boldsymbol{F} = 3000$ [N], the corners on the left side of the plate are fixed. However, due to condition (2), the loading forces were evenly distributed among the eight nodes in the lower right corner. The stress concentration at the fixed node in the upper left corner was reduced by adding seven forces ($7\ x\ 700$ [N]) in the negative direction of the x-axis at the nearest nodes at the edge of the plate. The stress concentration at the fixed node in the lower left corner was reduced by adding seven forces ($7\ x\ 700$ [N]) in the direction of the x-axis at the nearest nodes at the right edge of the plate and eight forces ($8\ x\ 375$ [N]) in the direction of the y-axis at the nearest nodes at the lower edge of the plate. Materials $(\mathbf{1},\mathbf{2},\mathbf{3},\mathbf{4})$ are used for optimization, and their parameters are shown in Tab. 2. The sizing for elements was used 2 [mm] with the total number of elements $N_E = 2958$ and 1 [mm] with the total number of elements $N_E = 10791$. The setting of MM ESO algorithm was $N_R = 10$, there was used AER ($\boldsymbol{N_\sigma} = 20$), the filter setting $R = 4$ [mm].

Total number of elements	Iteration Number	M [kg]	g [MPa]
2958	**240**	0.080	1.05
10791	**259**	0.080	1.89

Table 5. The effect of the total number of elements in Example 3 on the observed properties.

Fig. 8 a/ and Fig. 8 b/ show the decrease in the value of g and the change in the weight of the plate during the optimization, respectively.

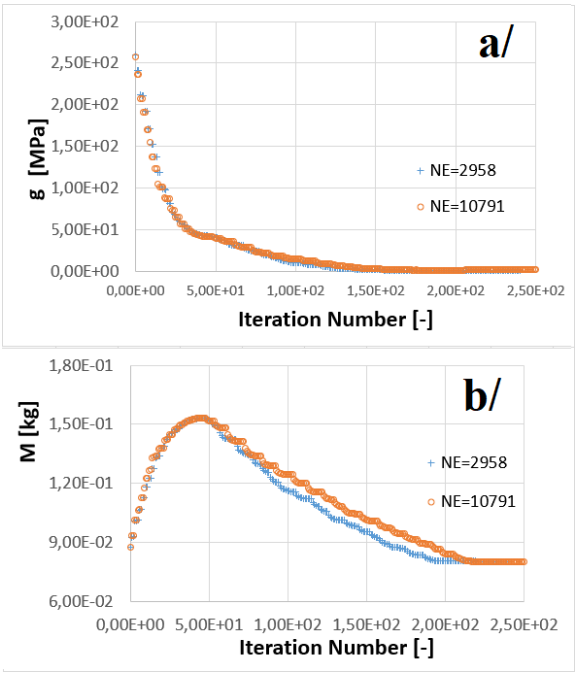

Figure 8. Example 3, evolution history for the objective function g and the structure weight M.

The final structure topology for different numbers of elements and their equivalent stresses are shown in Fig. 9.

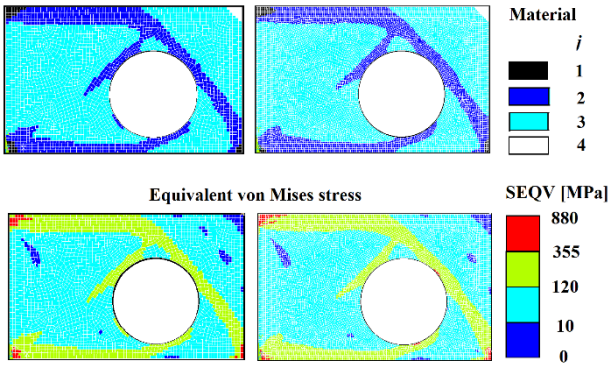

Figure 9. The last structure topology for two different meshes and their equivalent Von Mises stress [MPa].

5 DISCUSION

In the first example, an ER modification is tested. From Tab. 1, it can be seen, that the stress intervals for the individual materials are very different. The proposed modification (AER) divides all intervals into the same number of parts. It can be seen from Fig. 3 and Fig. 4 that a very similar structure was obtained in both but using AER with a much lower number of cycles. Therefore, AER modification was used in other examples.

In Example 2, the use of a mesh-independent filter was tested. The main difference is between ($R = 1$), when due to the size of the element, only one is selected and other variants. The differences between the other variants are negligible. The use of a filter simplifies the resulting topology of the structure and the filter is used in the last example.

In Example 3, the effect of the number of elements was tested. A very similar solution was obtained for the two tested variants, which is shown in Fig. 9. A complication for this step was the condition prescribed by Eqv. (2). These conditions required the correction of boundary conditions for all mesh changes. The results of the solution for five variants of the number of elements, where the adjustments of the boundary conditions were like those of Example 3 but without a more detailed description, are in Tab. 6. It can be seen from the table that the iteration number differs very little depending on the number of elements.

Total number of elements	Iteration Number	e-size [mm]	*g [MPa]*	*R [mm]*
217	174	8	6.65	9
829	189	4	1.00	5
2958	240	2	1.05	4
10791	259	1	1.89	4
37860	310	0.5	1.81	4

Table 6. The effect of the total number of elements in Example 3 on the observed properties.

Notes on the method :

- From Tab. 1 it is clear that the element stress for j-th material must not exceed $\boldsymbol{\sigma}^{\mathbf{1}}_{\mathbf{Max}}$, but the value lower than $\boldsymbol{\sigma}^{\mathbf{1}}_{\mathbf{Min}}$is permissible. This can be used to solve constraints.

- Eqv. (1) describes the difference from the ideal state and Eqv. (11) follows from this equation. Due to the termination criterion in the algorithm of Fig. 1, the last calculation may not satisfy equation (11).

- The material parameters **E**, **ρ** , **Re** do not have the same decrease gradient, see Tab. 2. This can complicate the use of displacement constraints.

6 CONCLUSIONS

The paper proposes an introductory modification of ESO algorithm for multiple materials. The MM ESO can be used for an initial design of a structure from multiple materials. The number of iterations is influenced more by the number of materials and other parameters of the method than by the number of elements. This method is not able to use any constraints, so our future work is to design an algorithm that includes displacement constraints.

ACKNOWLEDGMENTS

This article has been elaborated with the support of the project Research Centre of Advanced Mechatronic Systems, reg. no. CZ.02.1.01/0.0/0.0/16_019/0000867 in the frame of the Operational Program Research, Development and Education.

REFERENCES

[Paska 2020] Paska, Z. and Rojicek, J., Methodology of arm design for mobile robot manipulator using topological optimization. MM Science Journal, June 2020, pp 3918-3925, ISSN 1805-0476. https://www.mmscience.eu/journal/issues/june-2020/articles/methodology-of-arm-design-for-mobile-robot-manipulator-using-topological-optimization

[Krishna 2017] Krishna, L. S. R., et al. Topology optimization using solid isotropic material with penalization technique for additive manufacturing, Materials Today: Proceedings, 2017, Vol. 4, Issue 2, pp 1414-1422, ISSN 2214-7853. https://doi.org/10.1016/j.matpr.2017.01.163

[Qian 2020] Qian Chen, et al. A level-set based continuous scanning path optimization method for reducing residual stress and deformation in metal additive manufacturing, Computer Methods in Applied Mechanics and Engineering, 2020, Vol. 360, ISSN 0045-7825. https://doi.org/10.1016/j.cma.2019.112719

[Huang 2010] Huang, X., Xie, YM. A further review of ESO type methods for topology optimization, Structural and Multidisciplinary Optimization, 2010, Vol. 41, pp 671-683, ISSN 1615-1488. https://link.springer.com/article/10.1007/s00158-010-0487-9

[Han 2010] Han, D., Lee, H. Recent advances in multi-material additive manufacturing: methods and applications, Current Opinion in Chemical Engineering, 2020, Vol. 28, pp 158-166, ISSN 2211-3398. https://doi.org/10.1016/j.coche.2020.03.004

[®Ansys 2015] Ansys ®, inc. ansys release 16.01 documentation. https://www.ansys.com/, 2015. SAS IP, U.S.A.

[Xie 1993] Xie, Yi M., Grant P. Steven. A simple evolutionary procedure for structural optimization, Computers & structures, 1993, Vol. 49, pp 885-896, ISSN 0045-7949.https://doi.org/10.1016/0045-7949(93)90035-C

[Simonetti 2021] Simonetti, H. L., das Neves, F. D. A., Almeida, V. S., Multiobjective topology optimization with stress and strain energy criteria using the SESO method and a Multicriteria Tournament Decision, Structures, 2021, Vol. 30, pp. 188-197, ISSN 2352-0124. https://doi.org/10.1016/j.istruc.2021.01.002

[Wang 2016] Wang, N. F., Zhang, X. M. A solid isotropic material with parallel penalization method for structural topology optimization with multiple materials. In: International Conference on Manipulation, Automation and Robotics at Small Scales (MARSS), 18-22 July 2016, IEEE, pp. 1-6, ISBN 978-1-5090-1510-8. 10.1109/MARSS.2016.7561710

[Wang 2004] Wang, M. Y., Wang, X., "Color" level sets: a multi-phase method for structural topology optimization with multiple materials. Computer Methods in Applied Mechanics and Engineering, 2004, Vol. 193, pp. 469-496, ISSN 0045-7825. https://doi.org/10.1016/j.cma.2003.10.008

[Huang 2009] Huang, X., Xie, YM. Bi-directional evolutionary topology optimization of continuum structures with one or multiple materials. Computational Mechanics, 2009 , Vol. 43, pp 393-401, ISSN 1432-0924. http://dx.doi.org/10.1007/s00466-008-0312-0

[Rozvany 2009] Rozvany, G. I. A critical review of established methods of structural topology optimization. Structural and multidisciplinary optimization, 2009, Vol. 37, pp 217-237, ISSN 1615-1488. http://dx.doi.org/10.1007/s00158-007-0217-0

[Han 2021] Han, Y., Xu, B., Wang, Q., & Liu, Y. Bi-directional evolutionary topology optimization of continuum structures subjected to inertial loads. Advances in Engineering Software, 2021, Vol. 155, ISSN 0965-9978.https://doi.org/10.1016/j.advengsoft.2020.102897

[Gao 2020] Gao, Y., Ma, C., Feng, B., Tian, L. Bi-directional Evolutionary Structural Optimization of Continuum Structures with Multiple Constraints. In IOP Conference Series: Materials Science and Engineering, 2020, (Vol. 746, No. 1, p. 012043). IOP Publishing.http://dx.doi.org/10.1088/1757-899X/746/1/012043

CONTACTS:

Ing. Jaroslav Rojicek, Ph.D.
VSB -Technical University of Ostrava, Department of Applied Mechanics
17. listopadu 2172/15, Ostrava, 708 00, Czech Republic
+420 597 323 231, jaroslav.rojicek@vsb.cz, www.fs.vsb.cz/330